(Preprint) AAS 23-053

EXTENDED KALMAN FILTER PERFORMANCE ON THE ARTEMIS-1 MISSION

Jacob Sullivan[*] and Christopher D'Souza[†]

The Artemis Program is NASA's campaign to explore the Moon and beyond. Artemis-1, the uncrewed exoLEO test flight of the Orion spacecraft, was completed in 2022. There are four navigation Extended Kalman Filters (EKFs) that are part of the Orion navigation system. The Atmospheric Extended Kalman Filter (ATMEKF) estimates the vehicle position, velocity, and attitude (referred to as the vehicle state) during the ascent and entry phases of flight. Once Orion is outside of Earth's atmosphere, the Earth Orbit Extended Kalman Filter (EOEKF) and Cislunar Extended Kalman Filter (CLEKF) estimate the translational states, depending on the phase of flight, while the Attitude Extended Kalman Filter (ATTEKF) estimates the rotational state of the vehicle. The Kalman filters propagate the vehicle state forward in time using a combination of dynamics models and the output data from the Inertial Measurement Unit (IMU). The filters update the vehicle states and associated uncertainties, in the form of the covariance matrix, using pseudorange measurements from GPS (in ATMEKF/EOEKF), optical navigation measurements of the Earth or Moon (in CLEKF), and star tracker measurements (in ATTEKF). Simultaneously, the Kalman filters estimate error sources in the sensors, which are included in the state vectors as Exponentially Correlated Random Variables (ECRVs). This paper will summarize the performance of these filters during the Artemis-1 mission.

INTRODUCTION

The Artemis-1 mission launched from Kennedy Space Center on November 16, 2022 at 6:47:44 UTC aboard a Block 1 Space Launch System (SLS) rocket, with the objective of testing various systems of both SLS and the Orion spacecraft. After orbital insertion and a brief checkout in Low Earth Orbit (LEO), the Interim Cryogenic Propulsion Stage (ICPS) performed the Trans-Lunar Injection (TLI) burn, sending Orion on a trajectory for a lunar flyby 5 days later. After the Outbound Powered Flyby (OPF) burn, Orion inserted into a Distant Retrograde Orbit (DRO) and remained in the DRO for several days before performing the Return Powered Flyby (RPF) maneuver, sending the vehicle on a return trajectory to Earth. Orion re-entered the Earth's atmosphere at 17:20 UTC on December 11, 2022 and splashed down near Guadalupe Island off the Baja peninsula at 17:40:30 UTC, completing the 25-day test flight. Figure 1 provides an overview of the mission and trajectory.

The Orion Absolute Navigation (NVA) subsystem is unique with respect to many vehicle systems in that it is actively estimating the vehicle state throughout the entire mission, from prelaunch to post-landing. There is no time during which the vehicle is *not* navigating.

[*] Aerospace Engineer, EG/Aeroscience and Flight Mechanics Division, NASA Johnson Space Center, Houston, TX 77058
[†] Ph.D., Navigation Technical Discipline Lead, NASA Johnson Space Center, Houston, TX 77058

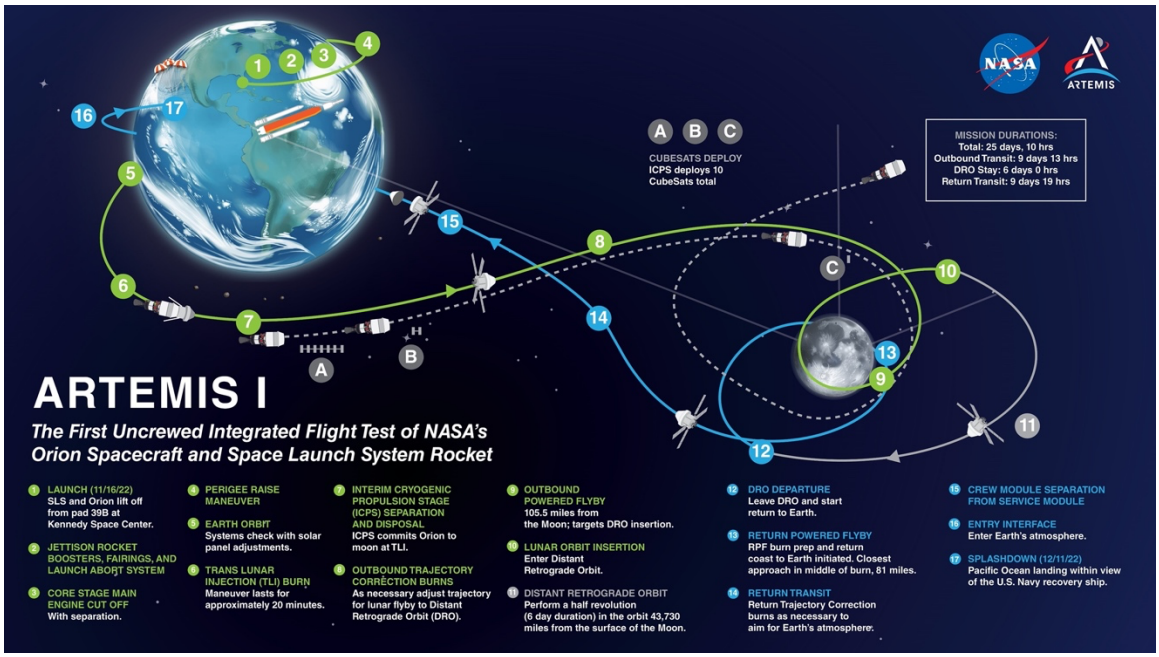

Figure 1. Overview of the Artemis-1 Mission.

To estimate the vehicle state throughout disparate mission phases with extremely different dynamic environments, the NVA subsystem uses four different versions of a Multiplicative Extended Kalman Filter (MEKF), which are active during different phases of flight. The attitude state is treated in a multiplicative (vis-à-vis an additive) fashion; in particular, the attitude is updated via a rectification process such that the attitude error state is rectified after each measurement. In point of fact, the attitude error state uses a scaled Modified Rodrigues Parameter (sMRP) representation. The quaternions in use in the filters are right-handed quaternions with a Hamiltonian composition. For prelaunch, ascent, and entry, the Atmospheric Extended Kalman Filter (ATMEKF) processes pad position and Global Positioning Satellite (GPS) pseudorange measurements. Due to the high dynamics and the baseline between the GPS antennae, ATMEKF can also estimate the vehicle attitude state. Once the vehicle is outside of Earth's atmosphere, NVA utilizes a split-filter design, where the Attitude Extended Kalman Filter (ATTEKF) processes star tracker measurements and the Earth Orbit Extended Kalman Filter (EOEKF) and the Cislunar Extended Kalman Filter (CLEKF) estimate the translational state using GPS and Optical Navigation (OpNav) measurements, respectively. The onboard translational filters are supplemented by state updates generated using orbit determination on range and doppler measurements from the Deep Space Network (DSN). This paper will present an overview of the NVA architecture, along with a preliminary analysis of the onboard navigation performance during the Artemis-1 mission.

ABSOLUTE NAVIGATION (NVA) ARCHITECTURE

The Orion sensor suite consists of three Orion Inertial Measurement Units (OIMUs), two GPS receivers, two star trackers, one OpNav camera, three barometric altimeters, and two sun sensor assemblies which are only used in Safe Mode. Figure 2 illustrates the sensor utilization across the mission phases. The raw measurements from each of these sensors are passed through a sensor-specific front-end data handler called the Subsystem Operating Program (SOP) before going to additional sensor-specific software which performs Fault Detection, Isolation, and Recovery (FDIR) checks to verify the sensor is operating properly and the measurements are fresh and valid.

This flow helps prevent any stale or erroneous measurements from being processed by the Kalman filters.

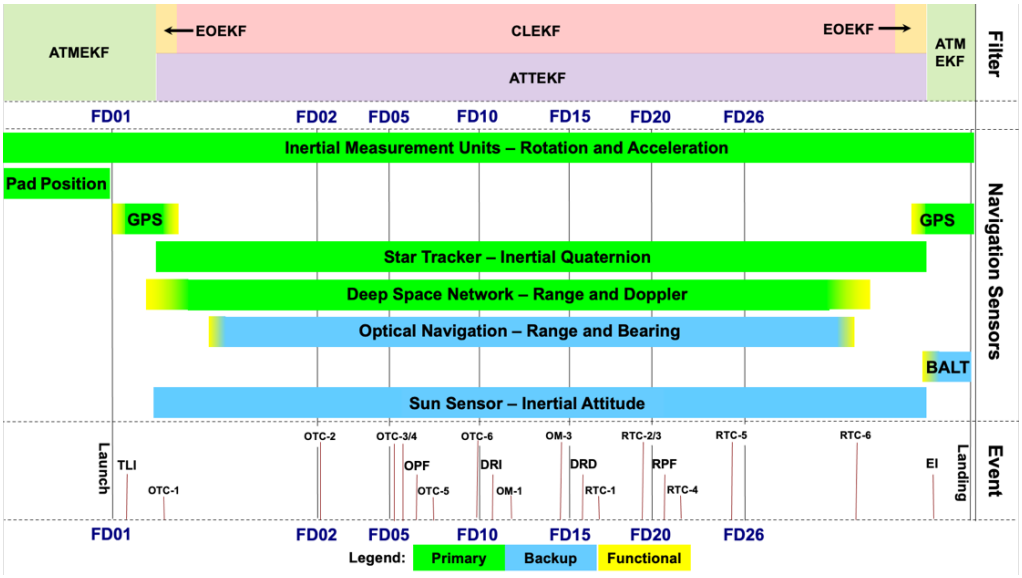

Figure 2. Sensor Utilization over Artemis-1 Mission Timeline.

Orion maintains four navigation channels during flight. The first three channels have identical algorithms and provide filtered navigation states; however, the inputs are from differing sensors. The usual (and well-established) navigation philosophy is utilized: the IMUs are being navigated in state-replacement mode. This means that the non-gravitational accelerations are not modeled; rather they are taken from the accelerometer outputs. For exo-atmospheric flight the accelerometer outputs are thresholded (or "gated") so as to not include accelerometer bias and noise when the thrusters are not firing. Similarly for the attitude state, only the attitude kinematics are modeled; the attitude dynamics are replaced by outputs of the attitude rate outputs of the gyros.

Channel 1 uses OIMU 1 and corrects the state with measurements from GPSR 1 and ST 1, while Channel 2 uses OIMU 2 and corrects with measurements from GPSR 2 and ST 2. Channel 3 uses OIMU 3 but utilizes the "best" available measurements both GPSRs and STs, as determined by the FDIR algorithms. Channel 3 is also the only channel which processes OpNav measurements, as certification of the OpNav algorithms was a Flight Test Objective (FTO) and the measurements were only to be used for primary navigation in the event of a permanent loss of communication with the vehicle. The fourth and final channel is the unfiltered channel, which propagates solely based off the vehicle dynamics and the DV/DTheta outputs from one of the OIMUs and is periodically re-synchronized with the state from one of the filtered channels throughout the mission. Figure 3 gives a visual representation of this architecture.

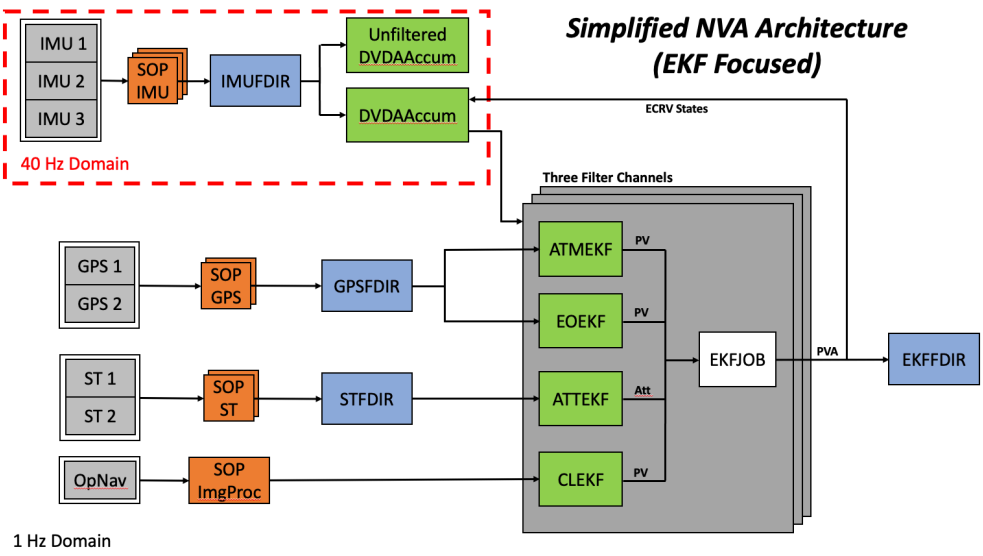

Figure 3. Overview of the EKF Inputs and Outputs.

PRACTICAL KALMAN FILTER IMPLEMENTATION CONSIDERATIONS

In practice, the classical Kalman filter equations are implemented in a more computationally efficient way. For the Orion navigation system, a UDU formulation following Bierman such that the estimation error covariance is factorized as $\mathbf{P} = \mathbf{UDU}^T$ where $\mathbf{U}$ is a unit upper triangular matrix and $\mathbf{D}$ is a diagonal positive definite matrix[1]. This formulation provides numerical stability, robustness to round-off error, ensures symmetry, and the ability to handle a positive semi-definite covariance matrix. To avoid costly matrix inversions, measurements are incorporated one-at-a-time using a Carlson rank-one update algorithm[2], and a hybrid Linear/Extended Kalman Filter update methodology, where the state update occurs only after all the measurements are processed, which allows the filters to be invariant to the order of the measurement processing.

Computational efficiency is obtained by partitioning the state space into two categories: (1) dynamics-driven states and (2) sensor parameters. The sensor parameters are modeled as Exponentially Correlated Random Variables (ECRVs) (or equivalently First-Order Gauss-Markov (FOGM) processes) and require tuning involving the selection of a time constant and parameter process noise. This partitioning allows for use of rank-one update for the covariance propagation. The UDU measurement update requires scalar updates (and decorrelated measurements); however, this is not a restriction because correlated measurements can be easily decorrelated by means of a transformation. Measurements are not so cooperative as to occur and be available at the filter propagation time; hence care is taken to process the measurements at the time they are made available in the filter. This involves a buffering of state data to be able to process latent measurements – up to a 3 second latency. Finally, any combination of the sensor parameters can be "considered" as necessary; the UDU framework has been modified to allow for this. The overall state process noise was tuned using extensive preflight Monte Carlo analyses.

The filters must protect against spurious measurements during operation. In general, the larger the measurement residual, the greater the effect of the measurement on the state estimate. The matrix inverse in the Kalman gain acts as a weighting function between the measurement noise variance $\mathbf{R}_k$ and the *a priori* estimation covariance $\mathbf{P}_k^-$. The residual will have a much greater effect if the state uncertainty $\mathbf{P}_k^-$ is large relative to the measurement noise variance, and conversely the residual will have little effect if the state uncertainty is on the order of the measurement variance.

The innovation variance $\mathbf{H}_k\mathbf{P}_k^-\mathbf{H}_k^T + \mathbf{R}_k$ may be used to monitor the health of the sensor and filter. If the measurement residual is greater than a parameterized factor times the standard deviation (square root of the innovation variance), the measurement is rejected or "edited" by the filter. Repeated rejections may indicate the sensor has failed or the filter has diverged.

Along with residual editing, the EKFs implement the Lear measurement underweighting scheme[3] for scenarios where a large *a priori* state uncertainty matrix incorporates a non-linear high-accuracy measurement, potentially causing the covariance to snap down too rapidly. This danger is particularly acute in light of the fact that the EKF formulation assumes that the linear portion of the Taylor series expansion is dominant. There are three times in the Artemis-1 mission where underweighting may be particularly necessary. During ascent, the GPS antennae are obscured by the Launch Abort System (LAS) while the navigation system is propagating the acceleration from the SLS. Once the LAS is jettisoned, accurate pseudorange measurements suddenly become available. The second occasion occurs when Orion is approaching the GPS constellation altitude near the end of the mission, when there is a potentially large state uncertainty from the long cislunar flight. Finally, the heat and plasma during re-entry causes a period of measurement blackout. Zanetti, DeMars, and Bishop note there are multiple possible implementations for measurement underweighting[4], on Orion underweighting is applied when the prior uncertainty, $\mathbf{H}_k\mathbf{P}_k^-\mathbf{H}_k^T$ exceeds a threshold and an underweighting correction is added to the measurement noise:

$$R_{UW} = R_k + \alpha\mathbf{H}_k\mathbf{P}_k^-\mathbf{H}_k^T \tag{1}$$

Translational EKF Implementation

For the translation states, the primary body's gravity field is modeled in terms of a 20X20 gravity field for Earth and an 8X8 for the Moon. In addition, the third body (Sun and Moon or Earth) is also modeled using a planetary ephemeris loaded before launch. The State Transition Matrix (STM) is computed using a first-order approximation to the STM and the gravity gradient matrix is computed just once – at the beginning of the interval. Additionally, the STM corresponding to the ECRV states are computed analytically. The STM partitions associated with the cross dynamics/sensor states are expanded in block-fashion and are computed carefully.

The ATMEKF is a coupled translation/rotation filter consisting of 40 states, which are listed in Table 1. Note that States 10-12 are shared between the GPS clock states and the pad position measurement error states since the two types of measurements are never incorporated at the same time. The first 13 states are considered dynamic states; states 14-40 are the ECRV states. Since the GPSR is a 12-channel receiver, 12 pseudorange states are included. This was a change made after EFT-1 in order to avoid the heavily time-correlated nature of the pseudorange measurements. For context, the EFT-1 navigation filter (from which the ATMEKF was derived) was a 28-state filter.

Table 1. Atmospheric EKF States

State Order	State Name	Dimension	Units
1 to 3	Vehicle Position	3	ft
4 to 6	Vehicle Velocity	3	ft/s
7 to 9	Vehicle Attitude Error	3	rad
10 to 13†	GPSR 1 and 2 Clock Bias and Drift	4	ft, ft/s
10 to 12†	Pad Position Bias	3	ft
14 to 16	Accelerometer biases	3	ft/s^2
17 to 19	Accelerometer Scale Factors	3	ND
20 to 22	Gyro Bias	3	rad/s
23 to 25	Gyro Scale Factors	3	ND
26 to 28	Gyro Misalignments	3	rad
29 to 40	Pseudorange Measurement Bias	12	ft

The EOEKF is a translation-only filter consisting of 28 states, which are listed in Table 2.

Table 2. Earth Orbit EKF States

State Order	State Name	Dimension	Units
1 to 6	Vehicle Position and Velocity	6	ft, ft/s
7 to 10	GPSR 1 and 2 Clock Bias and Drift	4	ft, ft/s
11 to 13	Attitude Error State	3	rad
14 to 16	Unmodeled Accelerations	3	ft/s^2
17 to 19	Accelerometer biases	3	ft/s^2
20 to 22	Accelerometer Scale Factors	3	ND
23 to 34	Pseudorange Measurement Bias	12	ft

Whereas the EOEKF is a translation-only filter, the attitude error state is needed to condition the covariance during translational maneuvers; this state is nominally not estimated (i.e., considered) in order not to have two filters (i.e., the EOEKF and the ATTEKF) in cascade.

The CLEKF is also a translation-only filter consisting of 28 states, which are listed in Table 3.

Table 3. Cislunar EKF States

State Order	State Name	Dimension	Units
1 to 6	Vehicle Position and Velocity	6	ft, ft/s
7 to 9	Attitude Error State	3	rad
10 to 12	Unmodeled Accelerations	3	ft/s^2
13 to 15	Accelerometer Biases	3	ft/s^2
16 to 18	Accelerometer Scale Factors	3	ND
19 to 21	Optical Navigation Biases	3	ND, ft

Attitude EKF Implementation

The ATTEKF is a rotation-only filter containing 12 states which are listed in Table 4.

Table 4. Attitude EKF States

State Order	State Name	Dimension	Units
1 to 3	Vehicle Attitude sMRP (IMU Case Frame $\mathcal{C}$)	3	rad
4 to 6	Gyro Bias (IMU Case Frame $\mathcal{C}$)	3	rad/s
7 to 9	Star Tracker 1 to IMU Misalignment (ST_1 Frame)	3	rad
10 to 12	Star Tracker 2 to IMU Misalignment (ST_2 Frame)	3	rad

FILTER PERFORMANCE

The performance of the filters across the various flight phases will be discussed chronologically. Table 5 provides a summary total of the total accepted and rejected measurement counts across the entire mission.

Table 5. Measurement Processing Across Artemis-1 Mission

	Channel 1		**Channel 2**		**Channel 3**	
Measurement Type	Accept	Reject	Accept	Reject	Accept	Reject
Pad Position	18,697	0	18,697	0	18,697	0
Ascent GPS	13,425	0	13,402	0	13,931	0
Outbound Orbit GPS	55,201	0	55,214	0	57,527	0
Star Tracker	>2M*	0	>2M*	0	>4M*	0
Optical Navigation	0	0	0	0	>700*	0
Inbound Orbit GPS	781	0	0	0	777	0
Entry GPS	16,101	0	10,902	0	17,051	0

Pad Position - Prelaunch

Before launch, the filters initialize by processing measurements of the surveyed pad coordinates mapped to the inertial frame. Since the vehicle is stationary with respect to the Earth-fixed frame, comparing the propagated state from the IMU measurements with the fixed surveyed position provides estimates of the pre-launch attitude errors and the IMU error ECRV states. The pad position biases in Table 1 are due to the survey error of the pad position. Figure 4 shows the measurement residuals for the pad position measurements, where the time axis is 0 at liftoff. The residuals are relatively small (within 0.1 feet in all axes for all channels) and after the early measurement processing appear normally distributed about 0.

* Precise count of total accepted measurements requires additional post-flight data processing

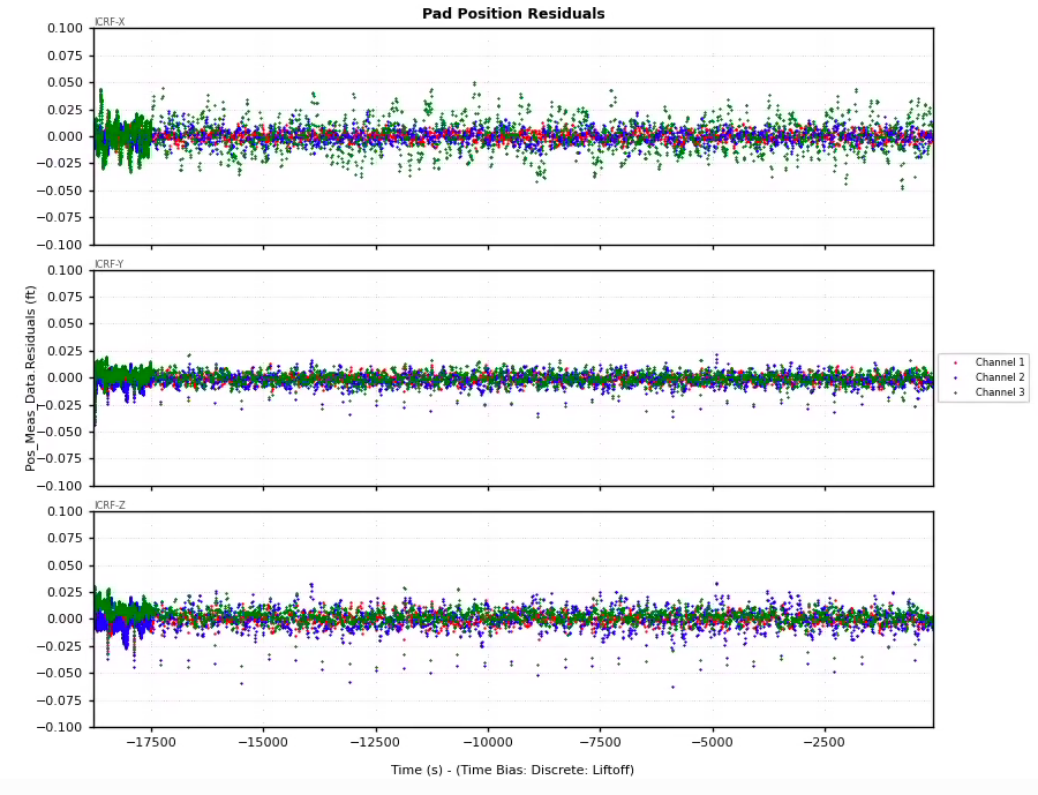

Figure 4. Artemis-1 Pad Position Measurement Residuals.

GPS Measurements – Ascent and Outbound Orbit

During the early portion of ascent, the Orion GPS antennae are covered by the LAS. Once the vehicle passes through the regime where an ascent abort may be necessary, the LAS is jettisoned and Orion is exposed to the environment. At this point, the two 12-channel GPS receivers begin acquiring signals and providing pseudorange measurements to the filters. As a reminder, for Artemis-1 while all three navigation channels have measurements from both GPS receivers available to them, the first navigation channel processes measurements from GPSR 1, the second channel processes measurements from GPSR 2, and the third channel processes measurements from both receivers, where the "best" measurements are selected by the GPS FDIR algorithms.

Figure 5 shows the GPS residuals and measurement counts during the ATMEKF phase of flight. The LAS jettison occurred about 207 seconds after liftoff, and the filters began processing GPS measurements within a minute of LAS jettison. The top subplot shows the residuals for Channel 1, the second shows residuals for Channel 2, and the third shows the Channel 3 residuals. GPSR 1 held signal throughout this phase of flight, while GPSR 2 had several brief dropouts, illustrated by the blue step chart in the second and third subplot. Overall, all three channels utilized between 5 and 12 satellites, and the residuals are well behaved, within tens of feet initially and decreasing as the filter had additional time to process. Figure 6 shows the pseudorange bias ECRV states for the ascent phase. Comparing this plot to Figure 5, once the residuals for a given satellite converge towards a steady-state value, the bias term also became stable, indicating the filter has allocated the residual error between the vehicle state and the satellite-specific bias term.

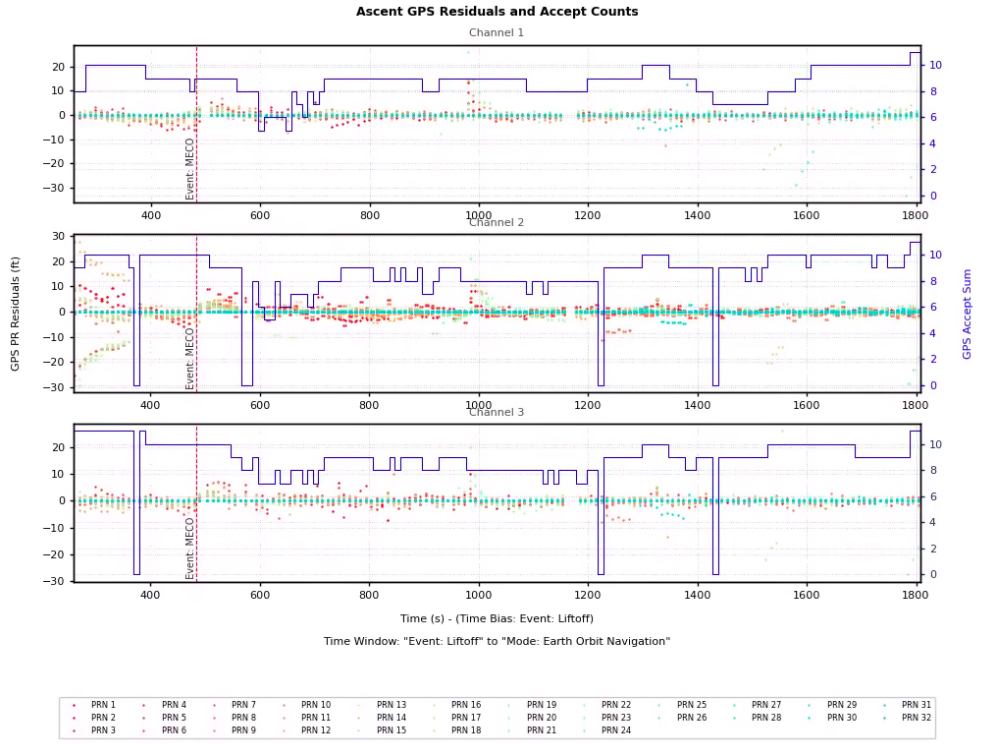

Figure 5. Artemis-1 Ascent GPS Measurement Residuals.

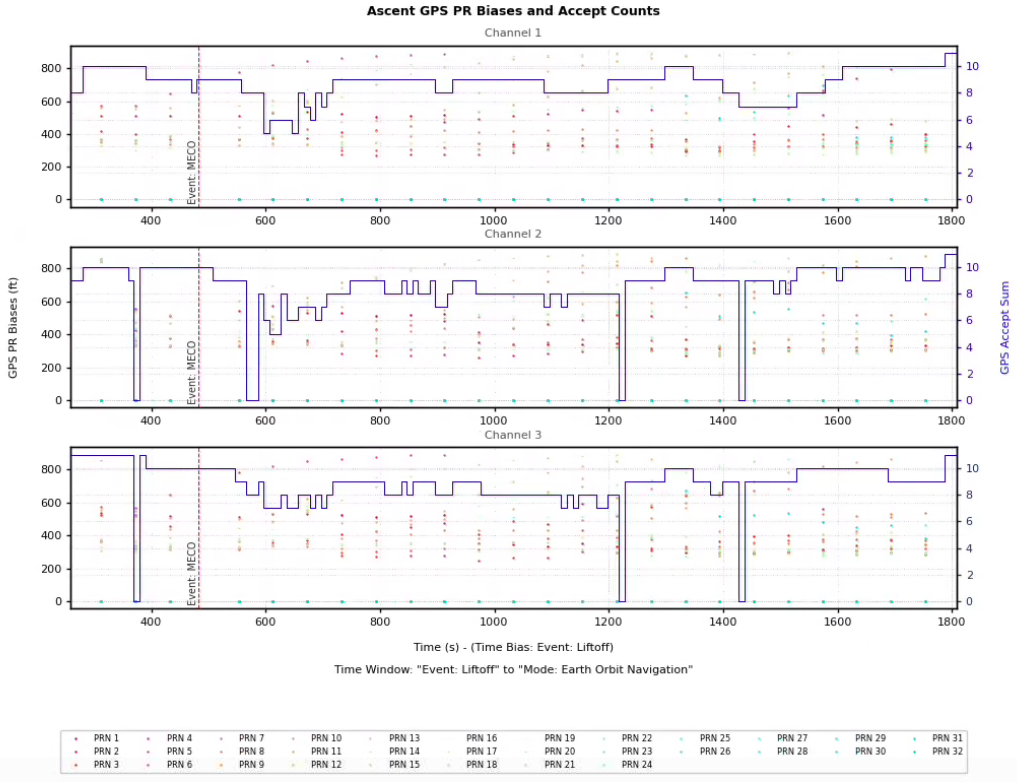

Figure 6. Artemis-1 Ascent GPS Pseudorange Biases.

Figures 7 and 8 show the residuals during the Earth Orbit phase and the associated pseudorange biases, respectively. This segment wass longer and had several significant events, particularly the Perigee Raise Maneuver (PRM), TLI burn, and the ICPS separation event. Once again, the residuals are well behaved through events, with all three channels processing between 6 and 12 measurements. There was a data dropout early in the Earth Orbit phase, however this does not affect the onboard processing. Residual excursions occur as new GPS satellites come into and exit the field of view, and the filters quickly incorporated the measurements and estimated the satellite-specific pseudorange biases in the ECRV states, as illustrated in Figure 8. After ICPS separation, the Orion GPSRs lost GPS satellites as the altitude increased, and the navigation system was moded to the Cislunar phase.

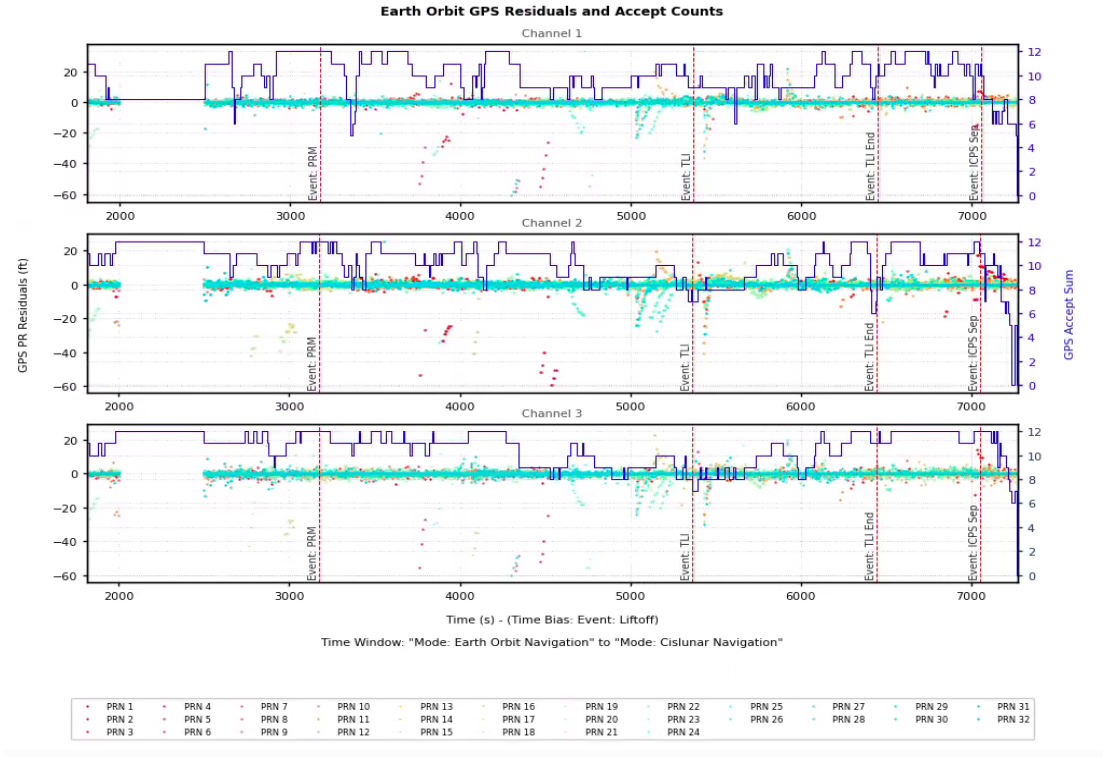

Figure 7. Artemis-1 Outbound Orbit GPS Residuals.

Star Tracker Measurements – Outbound Orbit

Figures 9 and 10 show the star tracker measurement processing during the same outbound phase of flight as figures 7 and 8, from the end of ATMEKF through the first several hours after liftoff. Notably, the star trackers did not begin processing until near the PRM, and Channel 2 did not process any measurements until after the PRM. There was some sporadic measurement processing before both units stopped processing prior to TLI, and the residuals grew to nearly 0.3 degrees over nearly an hour until after ICPS separation, when all three channels began processing measurements. Video analysis showed this was due to the clutter generated by the ICPS separation sequence when the star trackers couldn't identify the stars in their FOV due to the ICPS debris, causing the star trackers to report a high background noise. As the debris cleared, the residuals quickly snapped down, although there was another data dropout, this time due to radiation events likely caused by the transit through the van Allen belts. Figure 10 shows a zoom of the residuals to provide some scale for the magnitudes when the processing steadies out after around 10,000 seconds, and the

residual magnitudes remain within 0.01 degrees. From that point on, this residual magnitude was largely consistent throughout the mission.

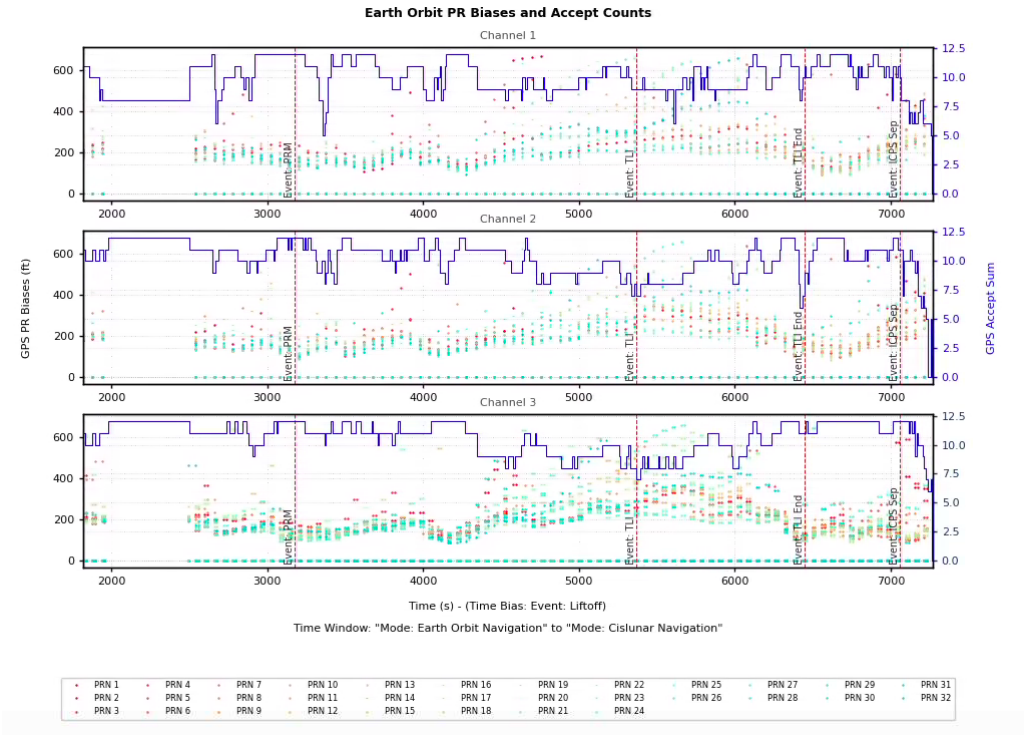

Figure 8. Artemis-1 Outbound Earth Orbit GPS Pseudorange Biases.

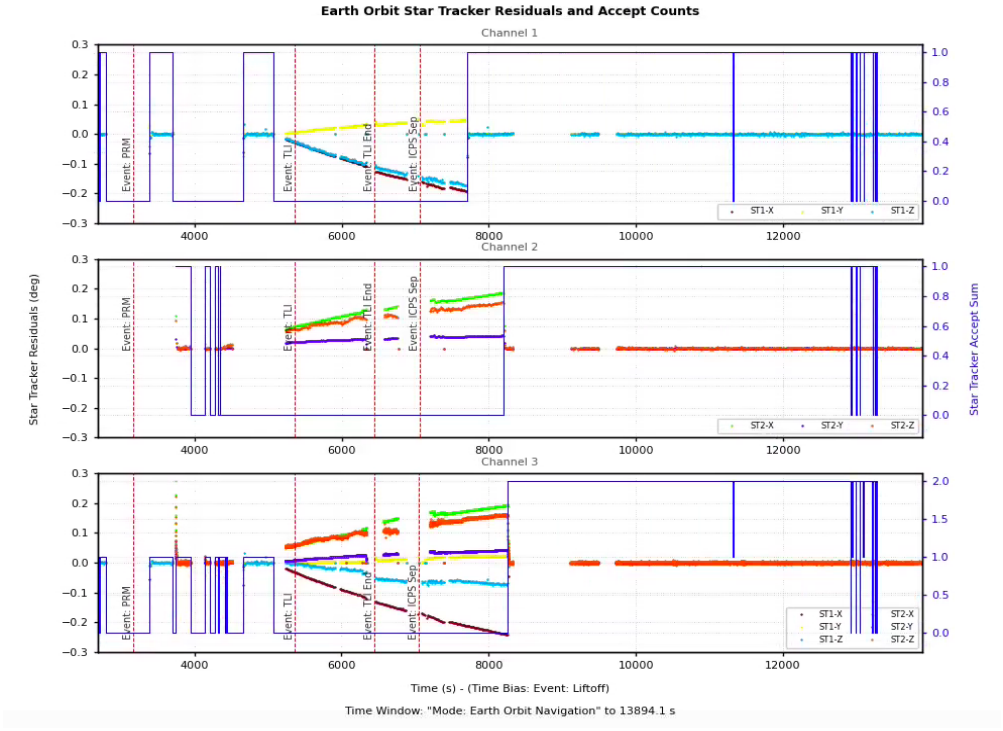

Figure 9. Artemis-1 Outbound Star Tracker Measurement Residuals.

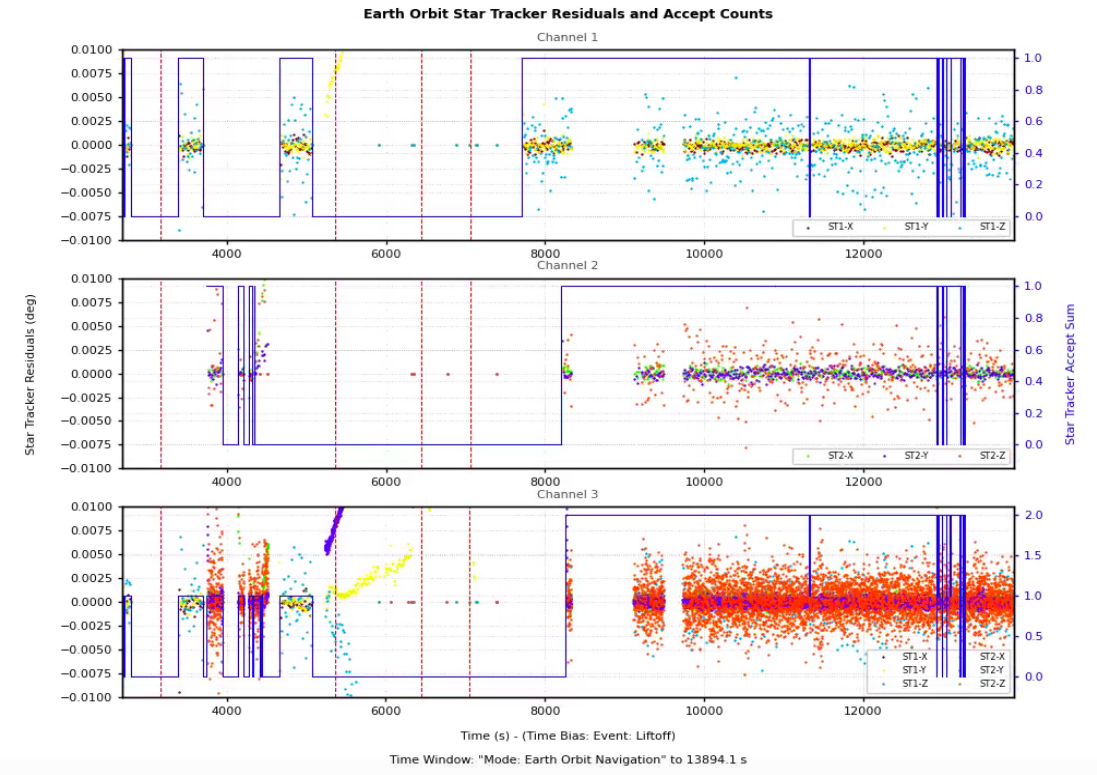

Figure 10. Zoom of Artemis-1 Outbound Star Tracker Measurement Residuals.

Optical Navigation Measurements

During cislunar flight the state is updated in one of two ways: a ground-based (DSN) update and an optical navigation update. The ground-based DSN update is not done via "measurement processing"; rather, the entire translation state and covariance is replaced in the CLEKF. The optical navigation update was done using onboard camera-based optical navigation measurements. These measurements were provided to the CLEKF from the camera controller which took the camera images which were then time-tagged and correlated with the ST-based quaternion and were then used to generate a set of angles (actually tangents of the angles, derived from the centroid of the planet) and a range measurement (derived from the apparent diameter of the planet).

Figure 11 depicts the measurement residuals for the first OpNav certification pass, which was a 2-hour long pass of the Earth on the first day of flight. From the figure, the initial bearing residuals were quite small, which indicates good attitude knowledge (and therefore an accurate pointing vector) from the star trackers, which follows from Figure 10. The bearing residuals started around 1 million feet and converged down over the first 1000 seconds of processing, and after roughly a half hour of imaging the range residuals became approximately distributed around 0, reaching the noise level of the measurement.

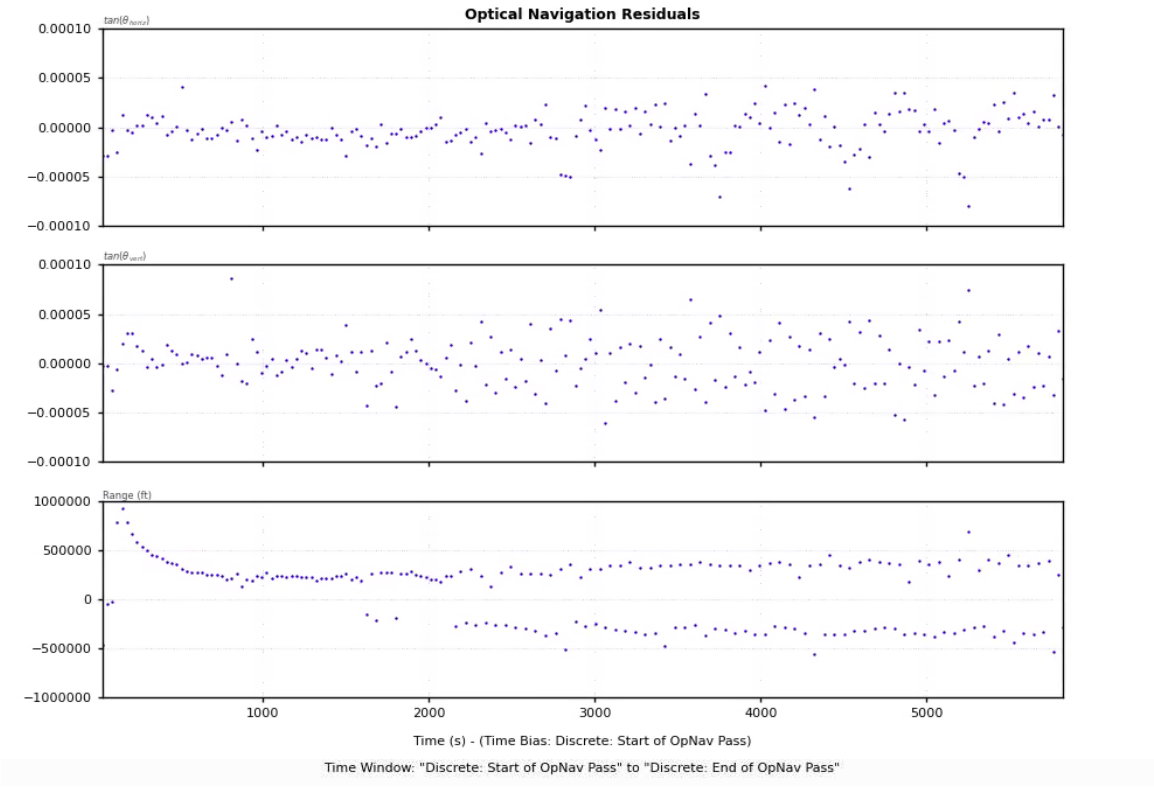

Figure 11. Optical Navigation Measurement Residuals for Earth Pass

Star Tracker Measurements – Inbound Orbit

The star tracker processing over the bulk of the mission was consistent and rather unremarkable, so the focus turns to the final day of flight. Figure 12 presents the star tracker residuals over the final day of flight, with Figure 13 showing the final phase before the navigation system transfers back to ATMEKF and star tracker measurements cease to be processed. Comparing Figures 12 and 13 to Figure 10, the residual magnitudes are consistent, around 0.01 degrees in all three axes. The scales are larger because measurements were not processed around the RTC-6 burn, marked by the red dashed line around 19,000 seconds to splashdown. Once ATTEKF resumed processing, the residuals quickly snapped back down to their noise levels.

Also of note in Figures 12 and 13 are the seemingly frequent star tracker "dropouts" which were present in all three channels, as indicated by the blue measurement accept sum lines. It was determined early in flight that these momentary drops were not due to any problems with the units or the navigation system. Rather, the plume from RCS firings from the attitude control system was visible and passing through the boresight direction of the sensors. These periodic firings caused the trackers to momentarily lose lock on the starfield and go back into acquisition mode. Since the units did not output any "bad" measurements while searching for an attitude solution, the filters simply did not process measurements during that time, rather than rejecting them.

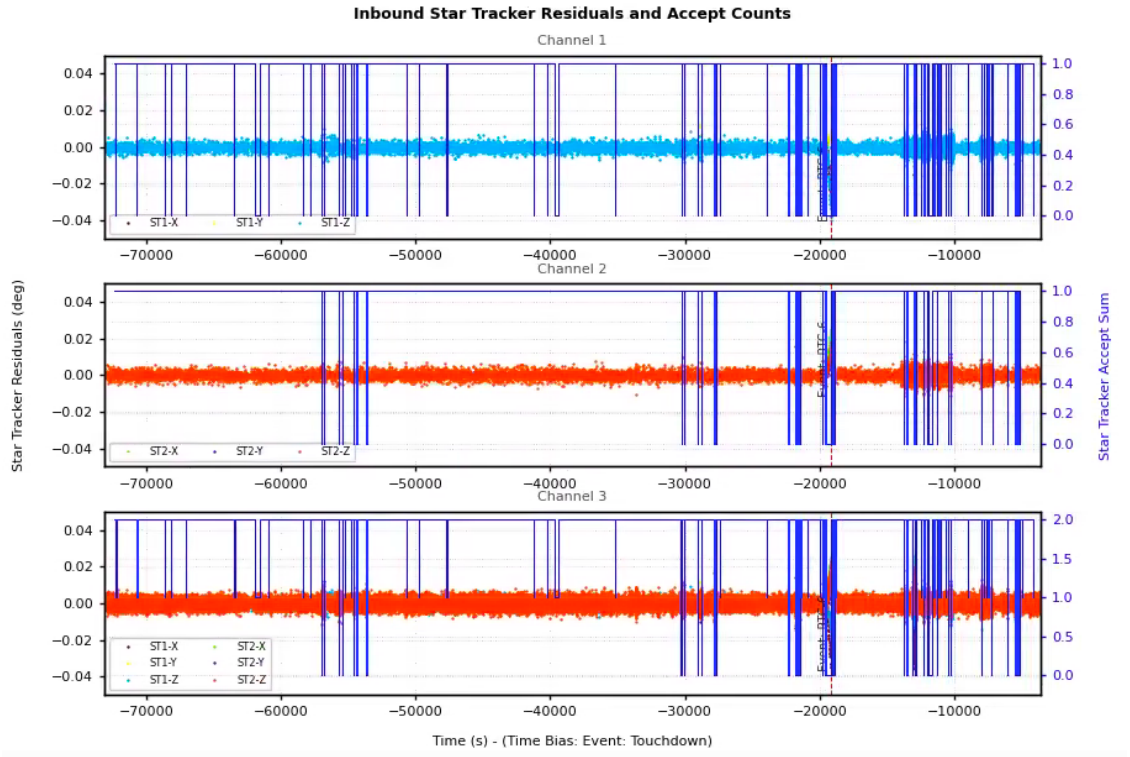

Figure 12. Star Tracker Measurement Residuals for Inbound Flight

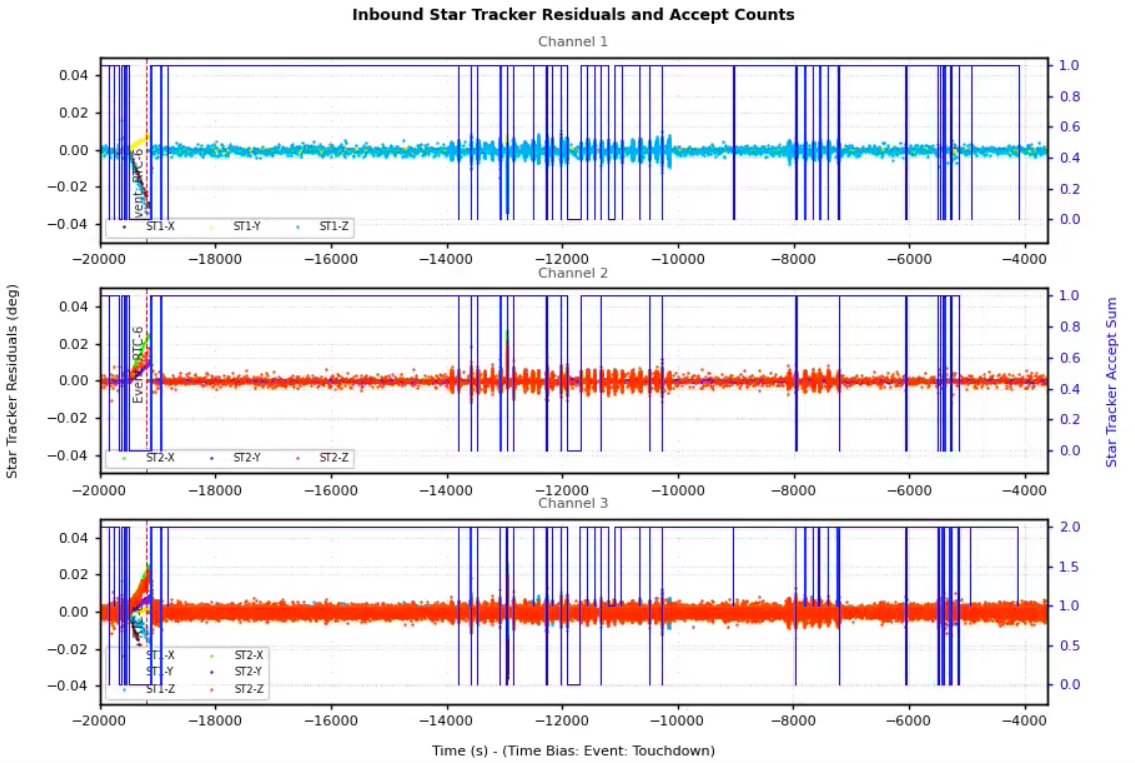

Figure 13. Star Tracker Measurement Residuals at End of Inbound Flight

GPS Measurements – Inbound Orbit and Entry

Orion moded back to EOEKF roughly 4,400 seconds prior to splashdown, to process any measurements which may become available as the vehicle passes inside the GPS constellation. Figure 14 shows the measurement processing during the inbound phase while navigation utilized EOEKF. Note that Channel 2 did not receive any measurements whatsoever during this phase, while Channels 1 and 3 (which both use GPSR 1 and its 2 associated antennae) picked up 4 measurements for approximately a minute around 4,100 seconds before splashdown, during which time the residuals began converging as the filter estimated the state. After a roughly 5-minute dropout, GPSR 1 again picked up 4 to 5 satellites before the transition to ATMEKF.

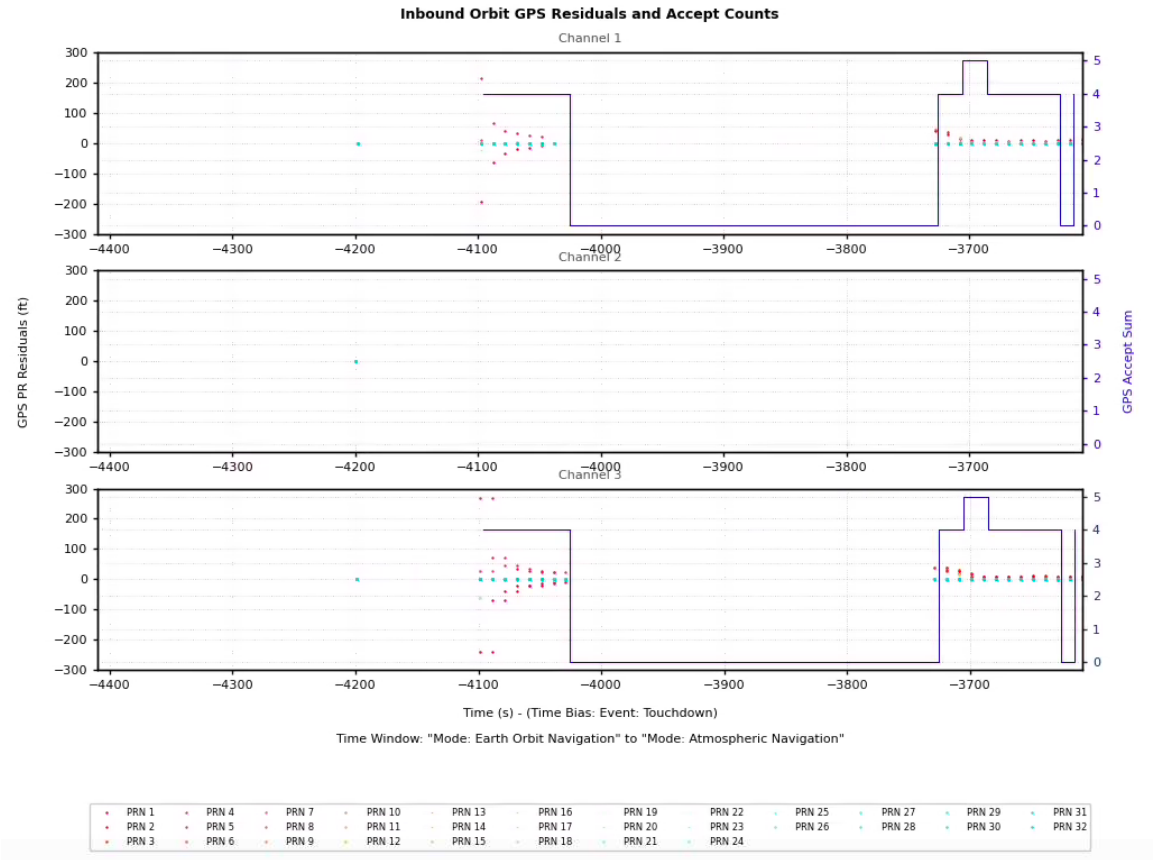

Figure 14. Artemis-1 Inbound Orbit GPS Residuals.

Once the vehicle transitioned to ATMEKF, GPS processing began in earnest. Channels 1 and 3 continued processing for approximately 10 minutes with the number of satellites increasing from 4 to 6 and up to 8 as shown in Figure 15. There was a dropout until after the Service Module separated and the Command Module performed the raise burn, and Channels 1 and 3 began processing between 7 and 12 measurements each. Channel 2 first acquired enough measurements after the CM raise burn, and all 3 channels processed until Entry Interface, when communication with the vehicle is lost. The blackout lasted longer than expected, with GPS measurements resuming around 5 minutes prior to touchdown, followed by a brief dropout and then successful processing until splashdown. Figure 16 presents the pseudorange bias states during the entry phase, and once again the states remained relatively stable during the prolonged periods of measurement processing.

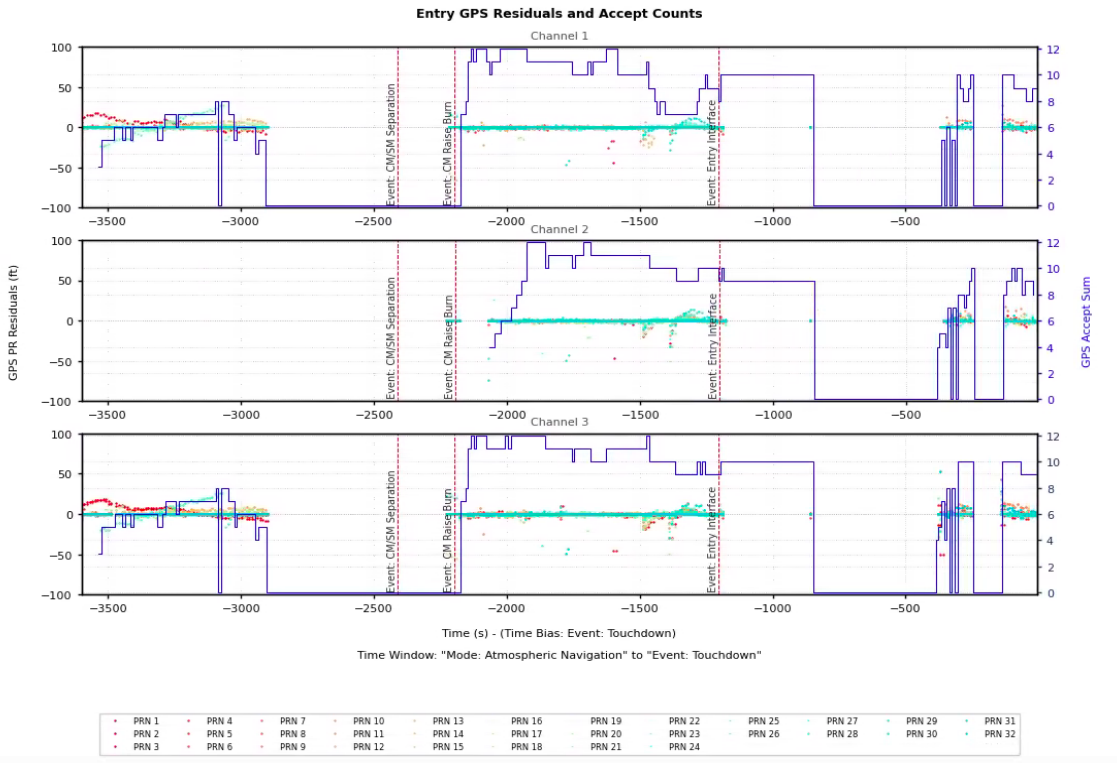

Figure 15. Artemis-1 Entry GPS Residuals.

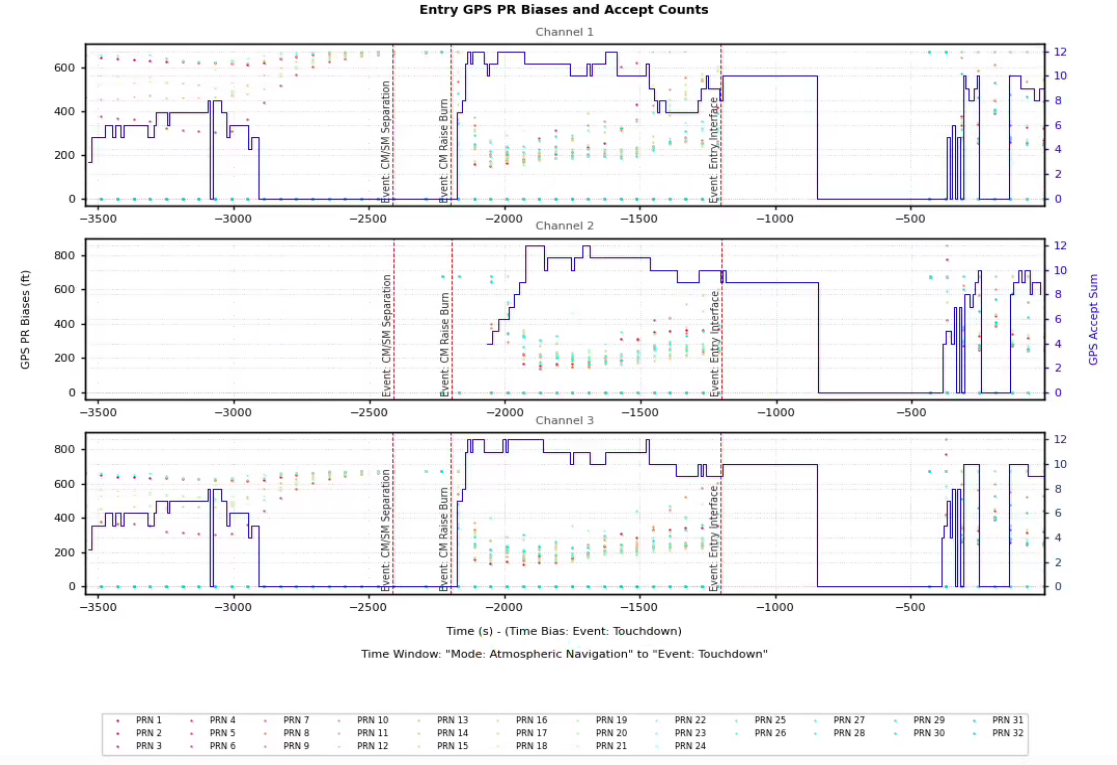

Figure 16. Artemis-1 Entry Pseudorange Biases.

CONCLUSION

Artemis-1 concluded its 25-day mission on December 11, 2022 with splashdown in the Pacific Ocean. The Orion Navigation Flight Software System performed magnificently during all phases of the Artemis-1 mission. Each of the four navigation EKFs processed measurements without issue and did not reject a single measurement. Despite a few growing pains associated with the star trackers during the initial portion of the flight, these issues did not resurface during the remainder of the mission. One of the previously untested systems (in a cislunar environment) was the optical navigation system, which was a FTO and was certified on the outbound leg before the first flyby maneuver. Even this system performed beyond the most optimistic expectations and was certified for the return leg in the event of a loss-of-communications with the vehicle (which obviously didn't occur).

The Artemis-1 flight test greatly increased confidence in the GN&C system for the first Artemis crewed mission, which is currently scheduled to occur in 2024.

ACKNOWLEDGMENTS

The list of contributors to the Orion absolute navigation MODE team who helped write, analyze, tune, test, and verify the navigation system over the years is too numerous to list here, but all deserve credit for their roles in returning a crewed spacecraft to the lunar vicinity. The authors would like to particularly acknowledge Dr. Renato Zanetti, Dr. Greg Holt, and Mr. Ellis King, who were instrumental in the software development of the Extended Kalman Filter CSUs

REFERENCES

[1] Bierman, G. J., "Factorization Methods for Discrete Sequential Estimation." *Mathematics in Science and Engineering,* Vol. 128, 241 pages. Academic Press, New York, NY, 1977.

[2] Carlson, N. "Fast Triangular Factorization of the Square Root Filter." *AIAA Journal*, Vol. 11, No. 9, 1973, pp. 1259-1268.

[3] Lear, W. M., "Multi-Phase Navigation Program for the Space Shuttle Orbiter," Internal Note No. 73-FM-132, NASA Johnson Space Center, Houston, TX, 1973.

[4] R. Zanetti, K. DeMars, and R. H. Bishop, "Underweighting Nonlinear Measurements," Journal of Guidance, Control, and Dynamics, Vol. 33, September-October 2010, pp. 1670–1675.